

Supporting Information

Role of Regeneration of Nanoclusters in Dictating the Power Conversion Efficiency of Metal-Nanocluster-Sensitized Solar Cells

Muhammad A. Abbas,^{†,‡} Rizwan Khan,^{†,‡} Seog Joon Yoon,^{¶,§} Jin Ho Bang,^{†,‡,§}*

† Nanosensor Research Institute, Hanyang University, 55 Hanyangdaehak-ro, Sangnok-gu, Ansan, Gyeonggi-do 15588, Republic of Korea

‡ Department of Bionano Technology, Hanyang University, 55 Hanyangdaehak-ro, Sangnok-gu, Ansan, Gyeonggi-do 15588, Republic of Korea

¶ Notre Dame Radiation Laboratory and Department of Chemistry and Biochemistry, University of Notre Dame, Notre Dame, Indiana 46556, United States

§ Department of Chemistry, Yeungnam University, Gyeongsan, Gyeongbuk-do 38541, Republic of Korea

§ Departments of Chemical and Molecular Engineering and of Applied Chemistry, Hanyang University, 55 Hanyangdaehak-ro, Sangnok-gu, Ansan, Gyeonggi-do 15588, Republic of Korea

AUTHOR INFORMATION

These authors equally contributed to this work.

Corresponding Author

*jbang@hanyang.ac.kr

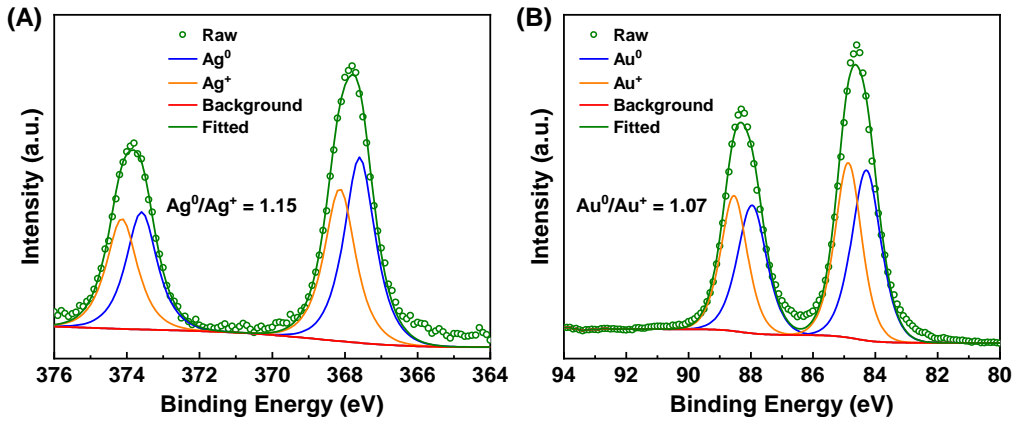


Figure S1. XPS spectra of (A) Ag NCs and (B) Au NCs along with the deconvolved peaks of neutral and oxidized metallic atoms. The ratios of Ag^0/Ag^+ and Au^0/Au^+ were determined to be 1.15 and 1.07, respectively.

Table S1. PL lifetimes of as synthesized Au and Ag NCs.^a

Sample	A_1	τ_1 (ns)	A_2	τ_2 (ns)	A_3	τ_3 (ns)	τ_{avg} (ns) ^b
Au NCs	0.58	2.14	0.27	35.19	0.15	346.00	292.57
Ag NCs	0.45	3.04	0.42	25.99	0.12	190.17	131.55

^a Lifetimes were calculated by fitting the PL decay traces to a tri-exponential function: $y = y_0 + A_1 e^{-x/\tau_1} + A_2 e^{-x/\tau_2} + A_3 e^{-x/\tau_3}$.

^b The average lifetimes were calculated using the following equation: $\sum A_i \cdot \tau_i^2 / \sum A_i \cdot \tau_i$.

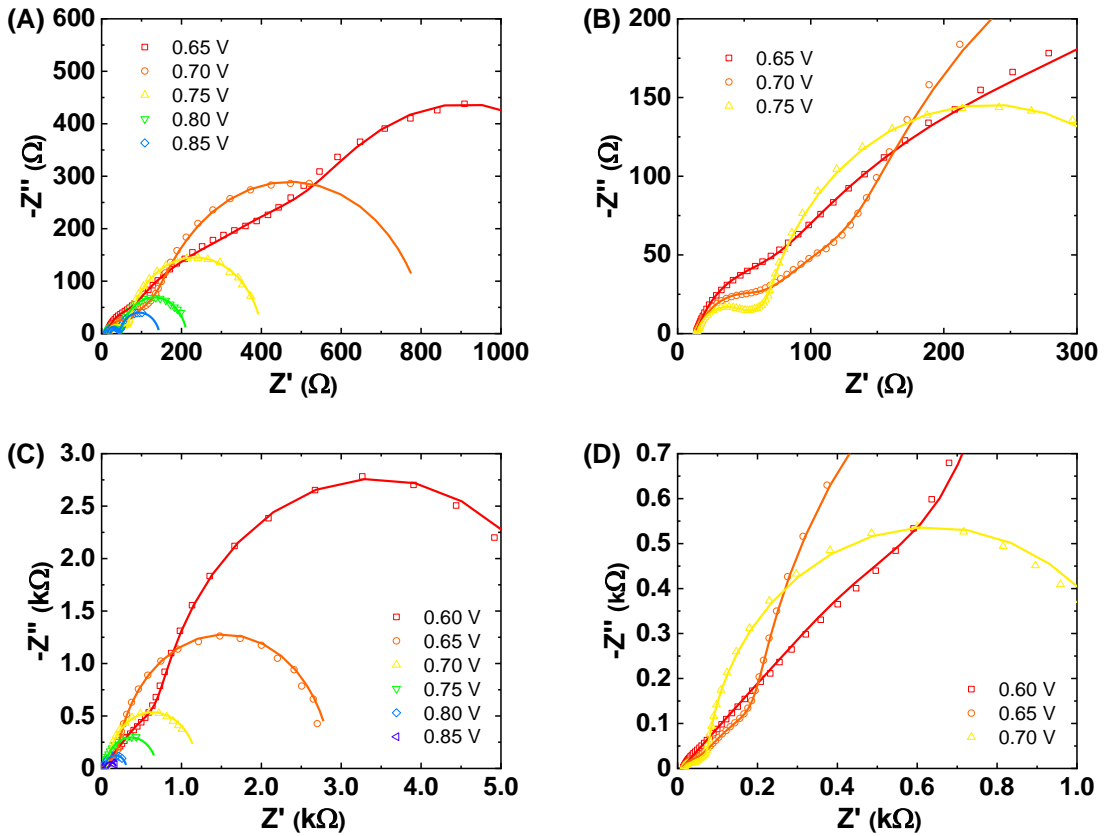


Figure S2. Nyquist plots of (A,B) Au-SSCs and (C,D) Ag-SSCs at different bias voltages. (B) and (D) are the zoom-in of (A) and (B) to show linear transmission lines.

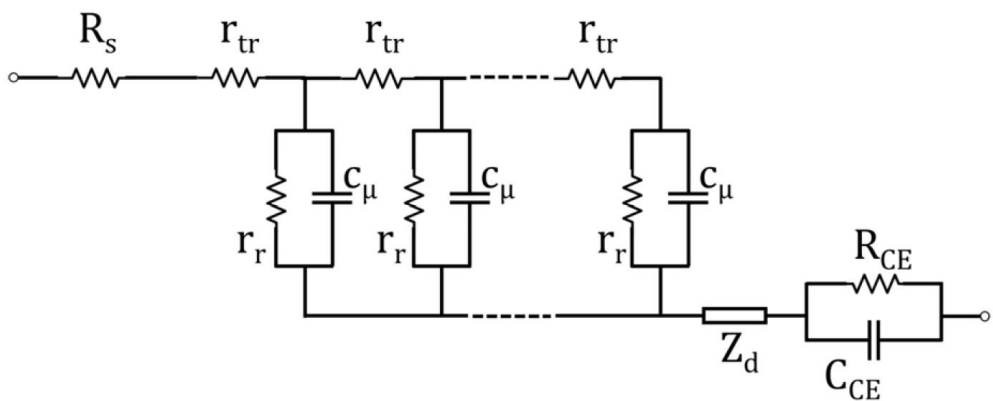


Figure S3. Transmission line model, as implemented in Gamry Echem software, used for fitting the Nyquist plots.¹ R_s is the series resistance, $R_r (=r_r \cdot L)$ and $C_\mu (=c_\mu \cdot L)$ are the recombination resistance and the chemical capacitance at the TiO₂/NC/electrolyte interface, respectively. Herein, L is the thickness of the TiO₂ film. $r_{tr} (=r_{tr} \cdot L)$ corresponds to the electron transport resistance through the

TiO_2 film which was calculated from the linear portion connecting the two semicircles. Z_d is the Warburg diffusion impedance of electrolyte, which is generally ignored during the fitting. R_{CE} and C_{EC} are the charge transfer resistance and the interfacial capacitance corresponding to the counter electrode/electrolyte interface. Copyright © 2016, American Chemical Society. Reprinted with permission.

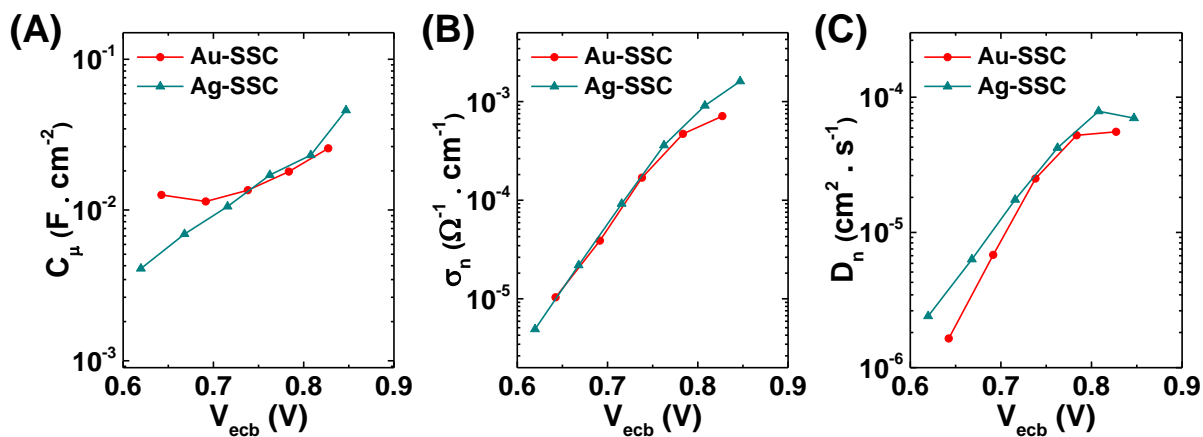


Figure S4. (A) Chemical capacitance (C_μ), (B) electron conductivity (σ_n), and (C) electron diffusion coefficient (D_n) as a function of equivalent conduction band voltage (V_{ecb}) for Au NC- and Ag NC-sensitized solar cells.

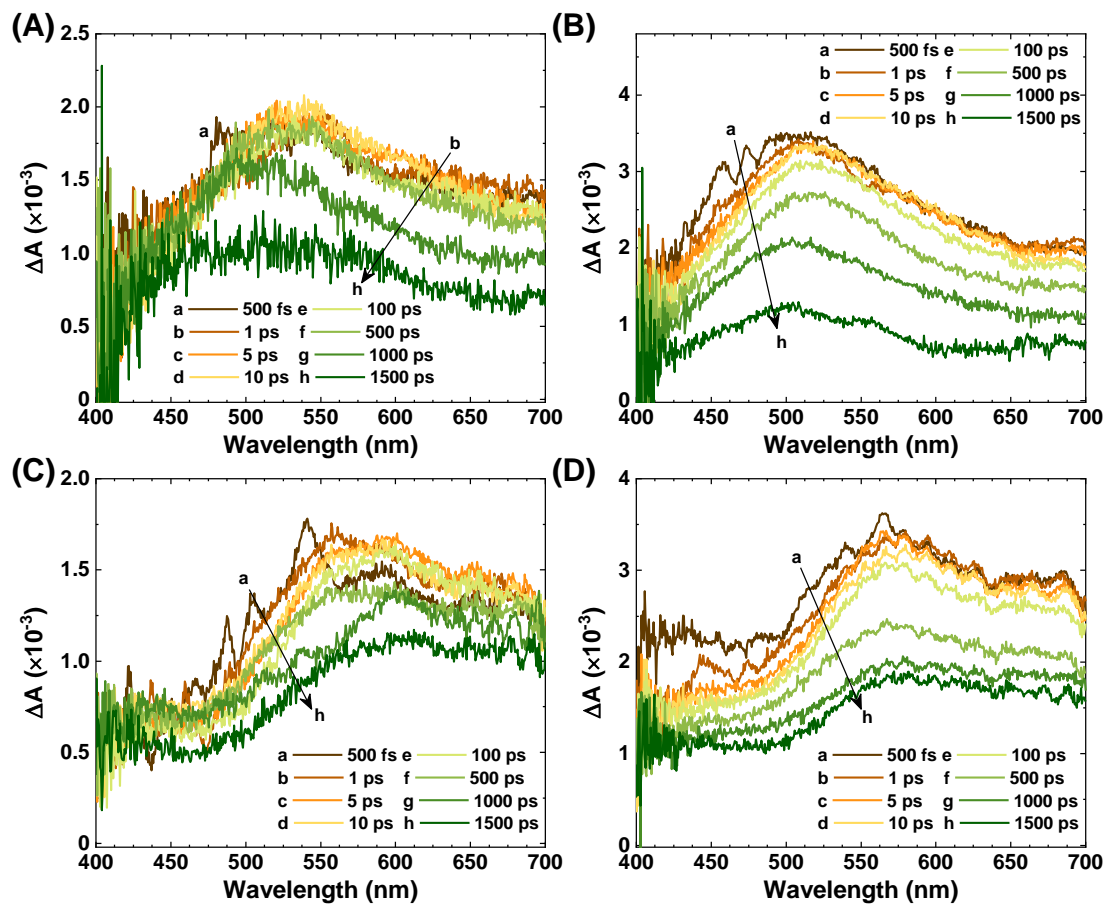
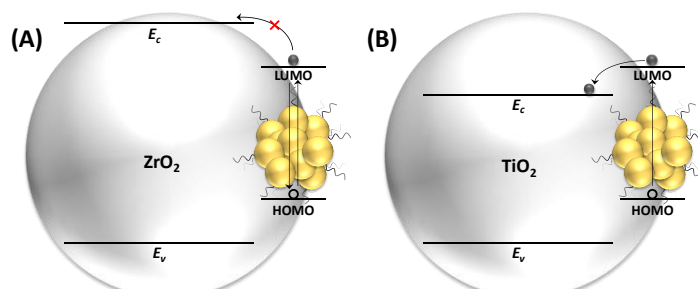


Figure S5. Difference absorbance spectra of Au NCs on (A) ZrO_2 and (B) TiO_2 at various time delays at the excitation wavelength of 387 nm. Difference absorbance spectra of Ag NCs on (C) ZrO_2 and (D) TiO_2 at various time delays at the same excitation wavelength.

Scheme S1. Photo-induced Electron Transfer from the LUMO Level of NC to the Conduction Bands of (A) ZrO_2 and (B) TiO_2 .



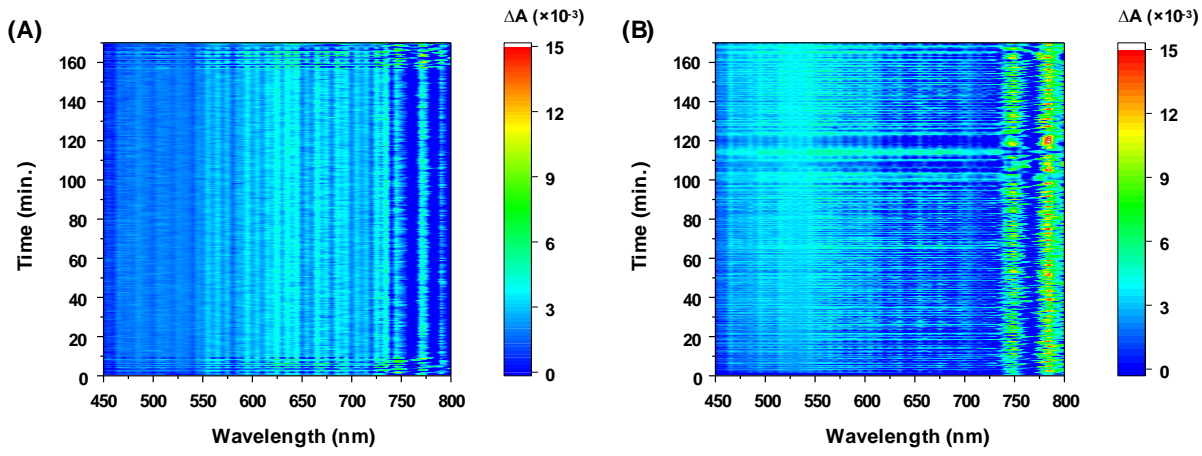


Figure S6. Time-resolved UV-vis absorption spectra of (A) Au NC- and (B) Ag NC-sensitized ZrO_2 films under continuous laser irradiation. The sample area was 0.4 cm^2 . The whole area was continuously exposed to continuous-wave laser radiation (405 nm) at a power of $182\text{ mW}\cdot\text{cm}^{-2}$ in ambient conditions. Changes in absorbance were measured every 20 s.

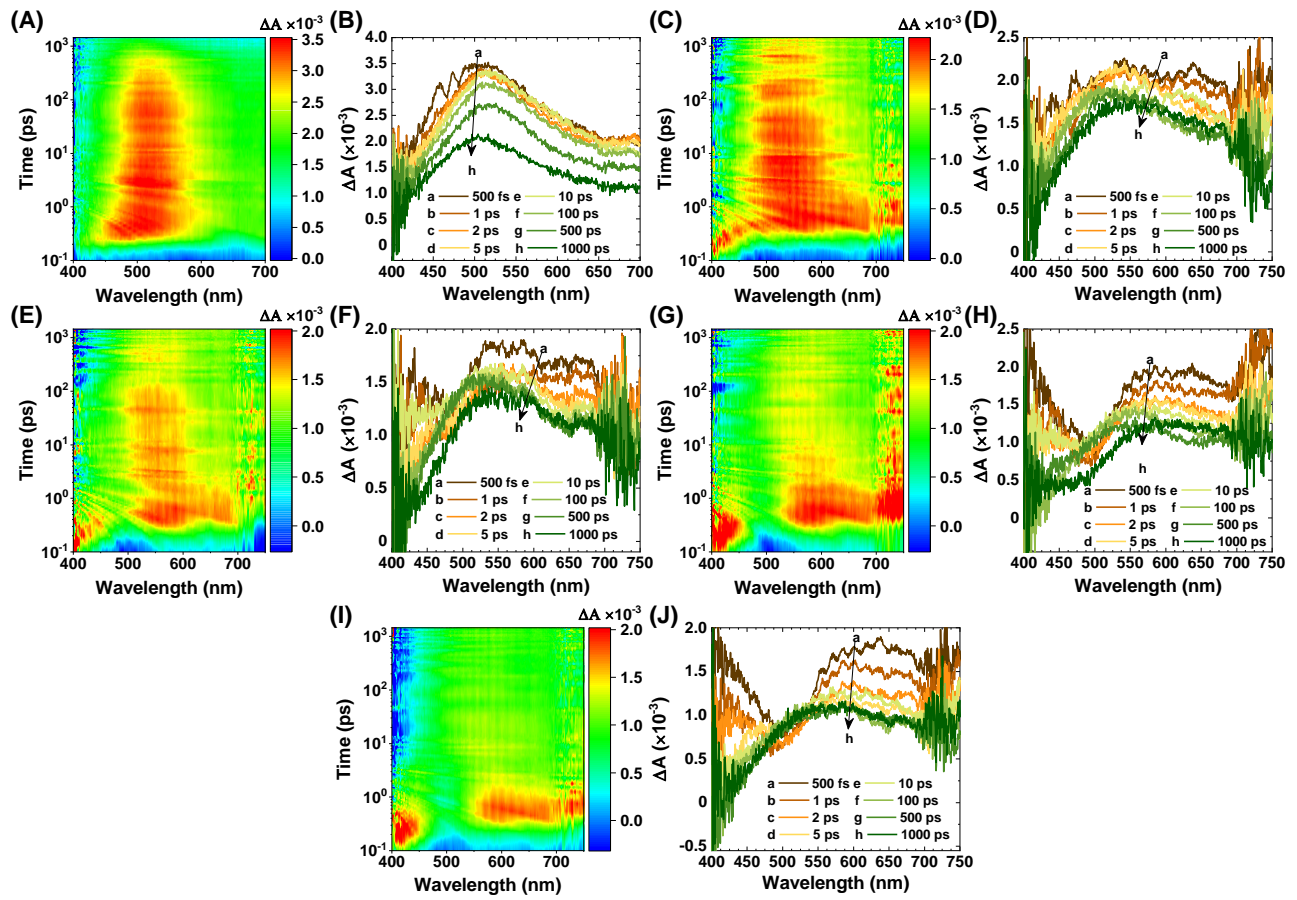


Figure S7. Transient absorption data maps and difference absorbance (ΔA) spectra of Au NCs adsorbed on TiO_2 after (A,B) 0 min, (C,D) 5 min, (E,F) 10 min, (G,H) 15 min, and (I,J) 20 min under continuous laser irradiation (387 nm and 30 $\text{mW}\cdot\text{cm}^{-2}$).

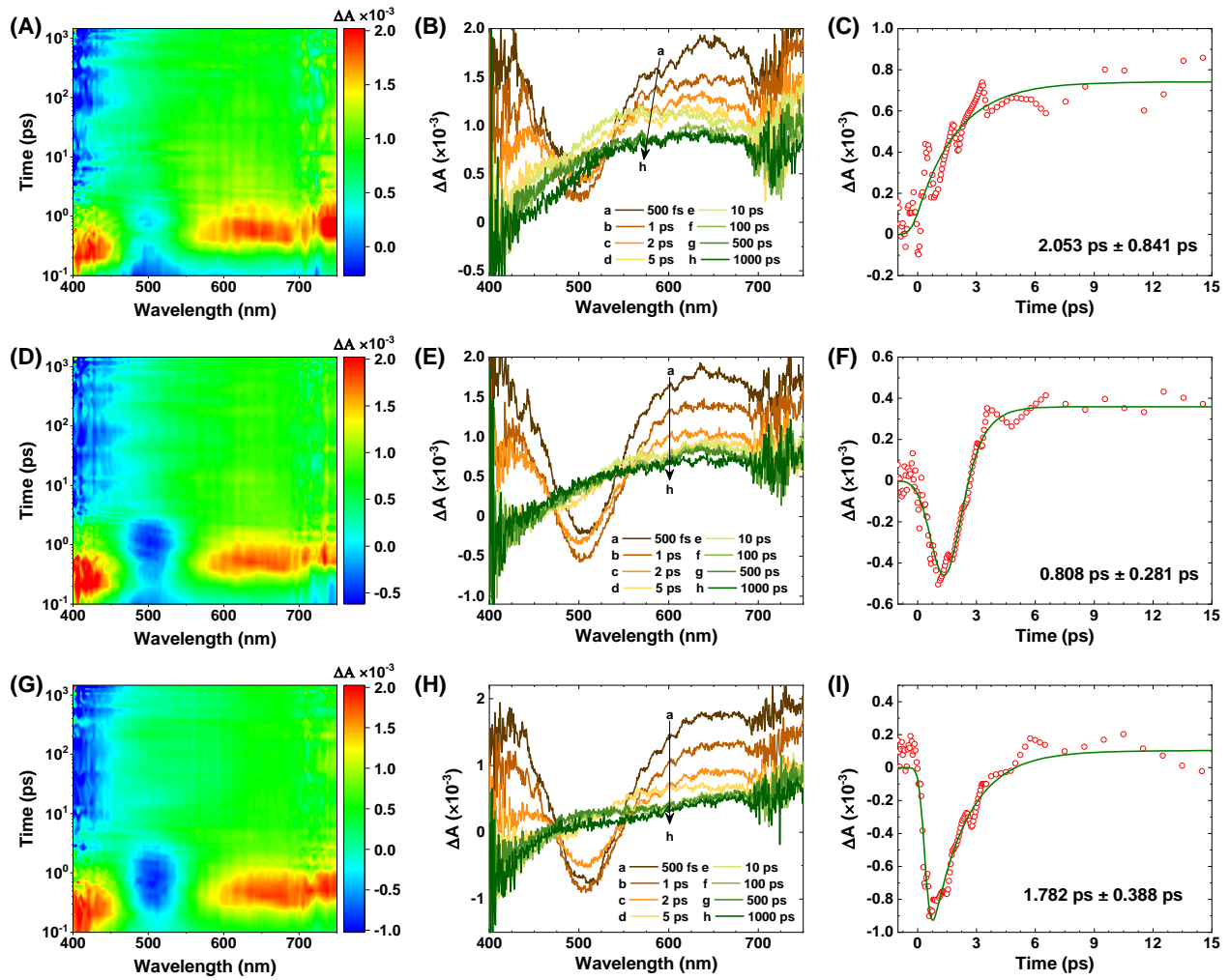


Figure S8. Transient absorption data maps and difference absorbance (ΔA) spectra (A-B, D-E, and G-H) and kinetics traces at 500 nm (C, F, and I) of Au NCs adsorbed on TiO₂ after (A-C) 30 min, (D-F) 60 min, and (G-I) 120 min continuous laser irradiation (387 nm and 30 mW·cm⁻²). The solid lines in (C, F, I) are mono-exponential fits to the kinetic traces in the corresponding figures. The appearance of bleaching signal at ~500 nm gives a clear indication of the formation of plasmonic nanoparticles.

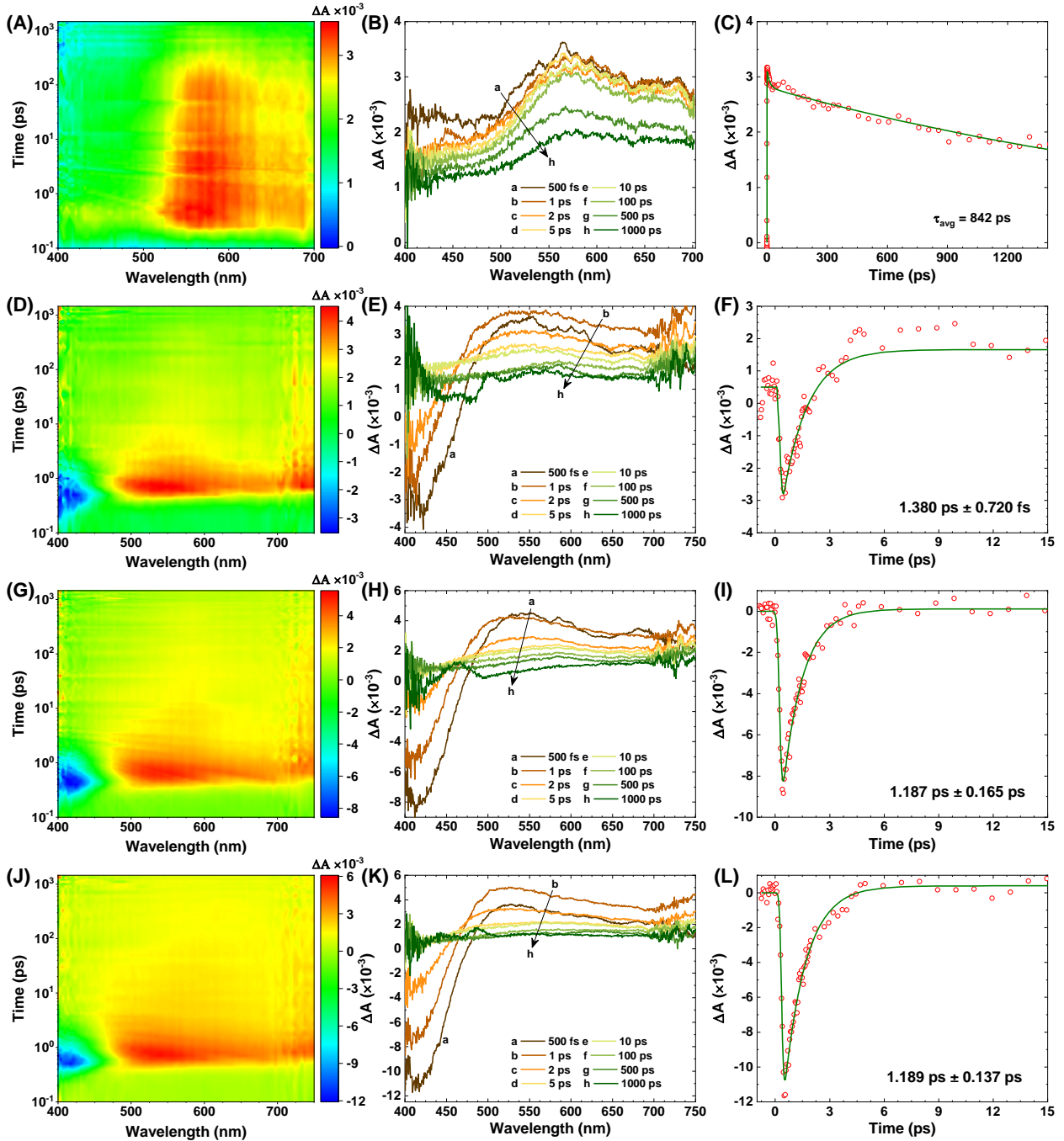


Figure S9. Transient absorption data maps and difference absorbance (ΔA) spectra (A-B, D-E, G-H, J-K) and kinetics traces at 605 nm (C) and 417 nm (F, I, L) of Ag NCs adsorbed on TiO₂ after (A-C) 0 min, (D-F) 5 min, (G-I) 10 min, and (J-L) 15 min of continuous laser exposure (387 nm and 30 mW·cm⁻²). The solid lines in (C, F, I, L) are mono-exponential fits to the kinetic traces in the corresponding figures. The appearance of bleaching signal at ~420 nm gives a clear indication of the formation of plasmonic nanoparticles.

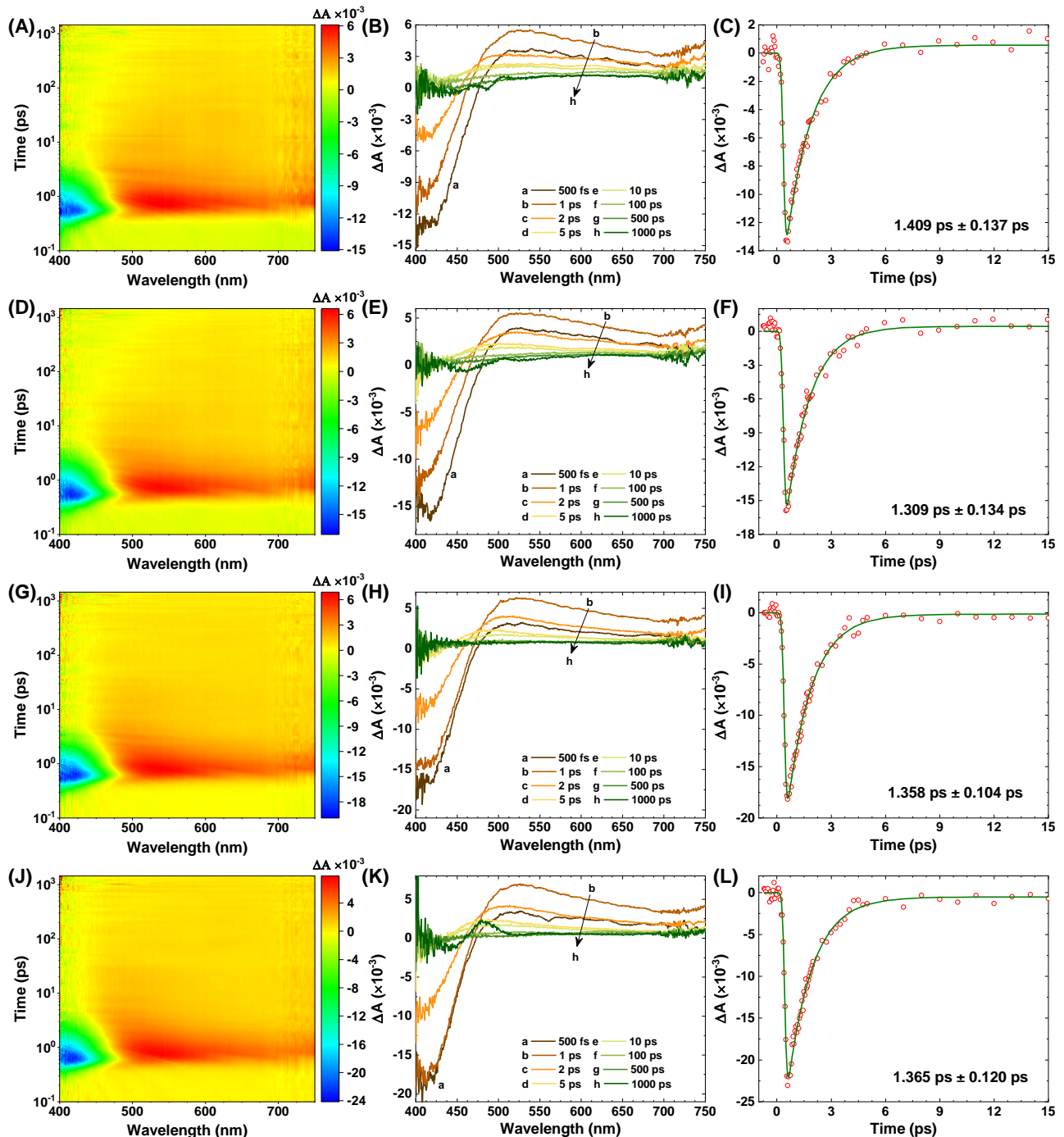


Figure S10. Transient absorption data maps and difference absorbance (ΔA) spectra (A-B, D-E, G-H, J-K) and kinetics traces at 417 nm (C, F, I, L) of Ag NCs adsorbed on TiO_2 after (A-C) 20 min, (D-F) 30 min, (G-I) 60 min, and (J-L) 120 min of continuous laser exposure (387 nm and $30 \text{ mW}\cdot\text{cm}^{-2}$). The solid lines in (C, F, I, L) are mono-exponential fits to the kinetic traces in the corresponding figures.

Reference

- (1) Abbas, M. A.; Kim, T.-Y.; Lee, S. U.; Kang, Y. S.; Bang, J. H. Exploring Interfacial Events in Gold-Nanocluster-Sensitized Solar Cells: Insights into the Effects of the Cluster Size and Electrolyte on Solar Cell Performance. *J. Am. Chem. Soc.* **2016**, *138*, 390-401.